



## Article

# Long-Term Stability of Novel Crucible Systems for the Growth of Oxygen-Free Czochralski Silicon Crystals

Felix Sturm <sup>1,\*</sup>, Matthias Trempa <sup>1</sup> , Gordian Schuster <sup>2</sup>, Rainer Hegermann <sup>2</sup>, Philipp Goetz <sup>2</sup>, Rolf Wagner <sup>3</sup>, Gilvan Barroso <sup>3</sup>, Patrick Meisner <sup>4</sup>, Christian Reimann <sup>1</sup> and Jochen Friedrich <sup>1</sup> 

<sup>1</sup> Fraunhofer IISB, Schottkystrasse 10, 91058 Erlangen, Germany

<sup>2</sup> CVT GmbH & Co. KG, Romantische Strasse 18, 87642 Halblech, Germany

<sup>3</sup> Rauschert Heinersdorf-Pressig GmbH, Bahnhofstrasse 1, 96332 Pressig, Germany

<sup>4</sup> SGL Carbon GmbH, Drachenburgstrasse, 53170 Bonn, Germany

\* Correspondence: felix.sturm@iisb.fraunhofer.de

**Abstract:** The replacement of the silica glass crucible by oxygen-free crucible materials in silicon Czochralski (Cz) growth technology could be a key factor to obtaining Cz silicon, with extremely low oxygen contamination  $< 1 \times 10^{17}$  at/cm<sup>3</sup> required for power electronic applications. So far, isostatic pressed graphite or nitrogen-bonded silicon nitride (NSN) crucible material, in combination with a chemical vapor deposited silicon nitride (CVD-Si<sub>3</sub>N<sub>4</sub>) surface coating, could be identified as promising materials by first short-term experiments. However, for the evaluation of their potential for industrial scale Cz growth application, the knowledge about the long-term behavior of these crucible setups is mandatory. For that purpose, the different materials were brought in contact with silicon melt up to 60 h to investigate the infiltration and dissolution behavior. The chosen graphite, as well as the pore-sealed NSN material, revealed a subordinated infiltration-depth of  $\leq 1$  mm and dissolution of  $\leq 275$   $\mu$ m by the silicon melt, so they basically fulfilled the general safety requirements for Cz application. Further, the highly pure and dense CVD Si<sub>3</sub>N<sub>4</sub> crucible coating showed no measurable infiltration as well as minor dissolution of  $\leq 50$   $\mu$ m and may further acts as a nucleation site for nitrogen-based precipitates. Consequently, these novel crucible systems have a high potential to withstand the stresses during industrial Cz growth considering that more research on the process side relating to the particle transport in the silicon melt is needed.

**Keywords:** Czochralski growth; silicon; crucible; oxygen concentration



**Citation:** Sturm, F.; Trempa, M.; Schuster, G.; Hegermann, R.; Goetz, P.; Wagner, R.; Barroso, G.; Meisner, P.; Reimann, C.; Friedrich, J. Long-Term Stability of Novel Crucible Systems for the Growth of Oxygen-Free Czochralski Silicon Crystals. *Crystals* **2023**, *13*, 14. <https://doi.org/10.3390/cryst13010014>

Academic Editor: Dah-Shyang Tsai

Received: 24 November 2022

Revised: 13 December 2022

Accepted: 18 December 2022

Published: 22 December 2022



**Copyright:** © 2022 by the authors. Licensee MDPI, Basel, Switzerland. This article is an open access article distributed under the terms and conditions of the Creative Commons Attribution (CC BY) license (<https://creativecommons.org/licenses/by/4.0/>).

## 1. Introduction

For some types of microelectronic devices, like insulated-gate bipolar transistors (IGBT), silicon wafers with significantly low oxygen contamination are indispensable [1,2]. Therefore, silicon crystals used for this application are typically grown by the Floating zone (Fz) technique, revealing an oxygen content far below  $1 \times 10^{16}$  at/cm<sup>3</sup> [3,4]. However, from an economical point of view, Czochralski (Cz) material would be preferred by electronic device manufacturers due to its lower process cost and the availability of larger crystal diameter up to 300 mm. The major drawback of the Cz technique is basically the limitation to silicon material with a significant increased oxygen content, typically higher than  $1 \times 10^{17}$  at/cm<sup>3</sup>. These examples of intense oxygen incorporation, even by application of an additional magnetic field (MCz), are mainly caused by melting up the silicon feedstock in the state of the art silica glass (SiO<sub>2</sub>) crucibles [4,5]. Hence, one promising approach would be the replacement of SiO<sub>2</sub> by oxygen-free crucible materials.

Only a few approaches to reduce the oxygen concentration during the Cz growth process by optimization of the crucible concept and materials were reported in literature during the 1980s. By application of a dense CVD-Si<sub>3</sub>N<sub>4</sub> coating on a SiO<sub>2</sub> glass crucible, Doi et al. could demonstrate a reduction of oxygen concentration to  $5 \times 10^{16}$  atoms/cm<sup>3</sup> [6].

Oxygen-free crucible systems were achieved by Watanabe et al. [7] and Matsuo et al. [8]. By graphite and Si<sub>3</sub>N<sub>4</sub>-based crucibles in combination with a CVD-Si<sub>3</sub>N<sub>4</sub> surface coating, the oxygen concentration in monocrystalline silicon ingots could be reduced below  $2 \times 10^{16}$  atoms/cm<sup>3</sup>. Nevertheless, due to the Si<sub>3</sub>N<sub>4</sub> coating dissolution by the silicon melt, it becomes saturated by nitrogen, which cannot be degassed from the melt. Consequently, nitrogen-related precipitates like Si<sub>3</sub>N<sub>4</sub> needles were formed by exceeding the nitrogen solubility limit of the melt [9]. By transportation of these particles to the solid–liquid interface and incorporation into the growing silicon ingot, an increase in dislocation density or even multi-crystalline growth occurred.

More recently, several new concepts for graphite [10–12] and Si<sub>3</sub>N<sub>4</sub>-based [13–18] crucibles for the growth of multi-crystalline silicon ingots were presented, which underlines the potential to use these materials in crucible setups during Si crystal growth.

In our previous work [19], we reconsidered this approach by evaluating several isostatic pressed graphite materials and nitride-bonded silicon nitride (NSN) in combination with a chemical vapor-deposited (CVD) Si<sub>3</sub>N<sub>4</sub> inner surface coating, according to their general applicability as crucible materials for Cz silicon growth. The crucible materials were characterized according to their performance and interaction with liquid silicon in lab scale melting experiments with moderate melt holding times up to 4 h.

However, considering the fact that, in an industrial Cz process the crucible is typically in contact with the silicon melt at much longer timescales ranging from ~30 h to >100 h, the knowledge about the long-term behavior and stability of the crucible setups is mandatory. For that purpose, so called dipping experiments as well as directional solidification (DS) runs were carried out with extended melt holding time up to 60 h. By detailed investigation of the dissolution behavior as well as the infiltration depth in combination with the resulting material morphology after the processes, the capability of the novel crucible setups to safely contain the silicon melt over long times scales was evaluated. Further, the minimum required thickness of the CVD-Si<sub>3</sub>N<sub>4</sub> coating should be discussed. Additionally, the DS crystallization experiments allowed the evaluation of the crucible behavior in contact with larger Si melt volumes over longer time scales and the Si ingot quality with respect to the formation of Si<sub>3</sub>N<sub>4</sub> based precipitates. In conclusion, the experimental results obtained in this work will help to further evaluate the use of these novel crucible setups during industrial Cz silicon growth processes and to identify which developments will still be necessary during perspective research.

## 2. Materials and Methods

For the dipping experiments, bare shaped NSN and graphite (blank and coated with CVD Si<sub>3</sub>N<sub>4</sub> coated) samples (65 × 40 × 10 mm<sup>3</sup>) were brought in direct contact with liquid silicon at defined process conditions for various time scales.

The NSN samples were achieved by the slip casting of a water-based slurry containing silicon powder (provided by Wacker Chemie AG, Munich, Germany) and Si<sub>3</sub>N<sub>4</sub> powder (provided by Alzchem Trostberg GmbH, Trostberg, Germany), followed by a heat treatment in nitrogen atmosphere. This method allows the formation of a Si<sub>3</sub>N<sub>4</sub> material with sufficient mechanical strength at relatively low temperatures about 1450 °C, but with an increased porosity up to 60%. For that reason, an additional pore sealing coating based on a polysilazane slurry [20,21] was developed and applied on the inner surface of NSN crucibles, finalized by a second nitridation step. For graphite samples, isostatic pressed material with low porosity and high mechanical strength (SGL Carbon GmbH, Wiesbaden, Germany) was used; hence, it has already shown excellent stability against the silicon melt in our previous tests [19].

The setup of the dipping experiments is described in Figure 1. In a first step, high purity silicon feedstock was melted in uncoated graphite crucibles (Ø 97/87 × 122 mm). The ratio of weighted silicon portion to the dipped surface of the NSN and graphite samples was chosen in that way, that it corresponds to the ratio of silicon volume to crucible contact

area in an industrial scale 32-inch Cz crucible setup. For CVD  $\text{Si}_3\text{N}_4$ -coated graphite samples, the ratio was doubled due to the only one-side coating.

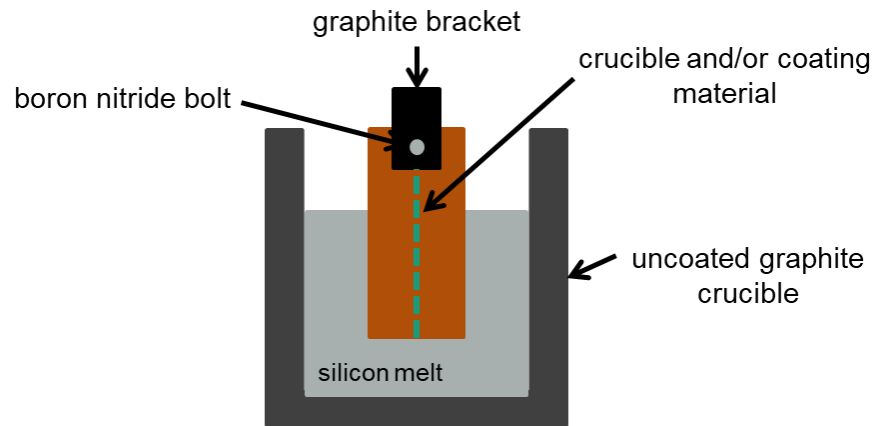


**Figure 1.** Schematic drawing of the experimental setup for investigating the dissolution of crucible and coating materials in liquid silicon. The dashed green line marks the preparation position of the vertical cross-section.

Furthermore, the chosen experimental setup excludes any kind of nitrogen contamination of the silicon melt, besides from the dipped materials itself. After a short melt homogenization period, the different samples were dipped into the silicon melt for 4 h, 8 h, 16 h, 25 h and 40 h. After the extraction from the melt, the liquid silicon in the crucible was crystallized in a directional solidification process. The dipped samples were treated with a solution of HF,  $\text{HNO}_3$  and  $\text{CH}_3\text{COOH}$  (volume ratio 6:81:13) to remove solidified silicon residues. After the etching and cleaning procedure, the dipped samples were embedded in epoxy resin, and vertical cross-sections were prepared. For the investigation of the dissolution of uncoated graphite vertical cross-sections were additionally cut from the crucibles after the dipping experiment. The resulting decrease of material/coating thickness and the infiltration depth of liquid silicon was determined by optical microscopy.

Besides the systematic investigation of the interaction with liquid silicon at small sample scale, the novel crucible setups were also tested in laboratory scaled DS silicon growth experiments. Therefore, crucibles ( $\text{Ø } 121.5/106.5 \times 110 \text{ mm}$ ) with a spherical bottom design in various configurations were prepared to evaluate their potential for Cz application (see Figure 2).

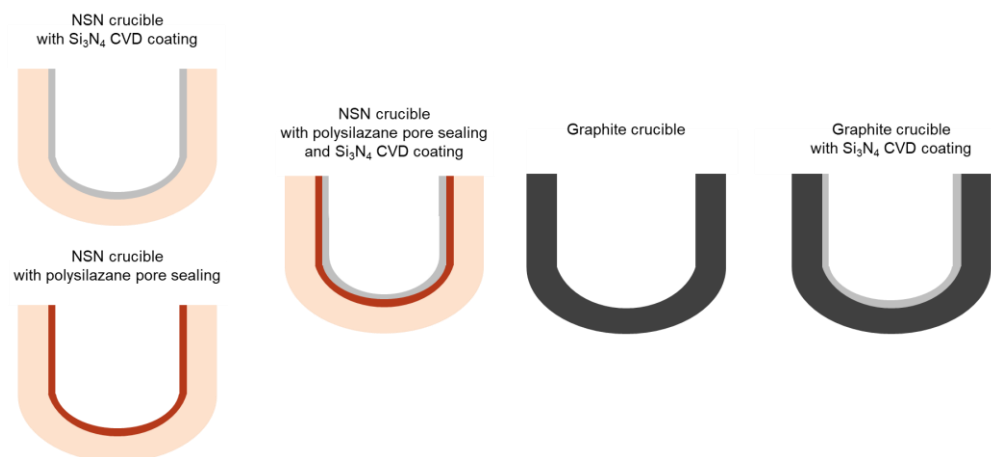


**Figure 2.** Overview of investigated crucible setups for oxygen-free Cz silicon ingot growth.

NSN-based crucibles were produced analogously to the NSN dipping samples. Additionally, the inner surface of the crucibles was covered either with a CVD  $\text{Si}_3\text{N}_4$  coating, a pore sealing coating  $\text{Si}_3\text{N}_4/\text{Si}/\text{polysilazane}$  (70/18/12 wt.%) or a combination of both. Further, isostatic pressed graphite crucibles, which have already shown good resistance against melt infiltration in our previous investigations [19], were used in uncoated and CVD-coated variants.

The averaged CVD  $\text{Si}_3\text{N}_4$  coating thickness on graphite crucibles was determined to be  $150\ \mu\text{m}$  at the crucible wall to  $>400\ \mu\text{m}$  at the bottom, while for NSN crucibles, it was  $170\ \mu\text{m}$  at the walls to  $>700\ \mu\text{m}$  at the bottom. The increasing coating thickness towards the crucible bottom is caused by the high reactive precursor gases and the geometric limitation of gas flux conditions during CVD application. The CVD coating reveals a good wear resistance, which allows the handling of the crucible without delamination or chipping of the coating.

The crucibles were heated up in vacuum conditions, and the silicon was melted within a period of 6 h. Afterwards, the liquid silicon was contained up to 60 h at 20 mbar in the different crucible setups, followed by a 7 h crystallization step (growth rate = 1–1.5 cm/h). After silicon solidification, 2 mm thick vertical slices were cut out of the center of the crucible as well as from the Si crystal. The crucible parts were etched analogously to the dipping samples to remove attached silicon and to expose the remaining CVD coating. The characterization of the structure and morphology of the CVD coating was carried out by optical and scanning electron microscopy (SEM).

Furthermore, the silicon samples were investigated by infrared (IR) transmission microscopy to observe the particles and precipitates formed in the silicon crystal.

### 3. Results and Discussion

#### 3.1. Dipping Experiments

For investigation of the infiltration behavior of liquid silicon in the coating and crucible materials at long time scale, dipping experiments with a variation of contact time to the silicon melt (4 h up to 40 h) were performed. Among others, this is important, hence the Si infiltration in C-based materials results in a silicon carbide (SiC) formation inducing a volume increase, which can lead to an intense crack formation in graphite materials with minor mechanical strength [19,22]. The resulting averaged infiltration depth, which was measured at vertical cross-sections through the various kinds of dipped samples, is summarized in Figure 3.

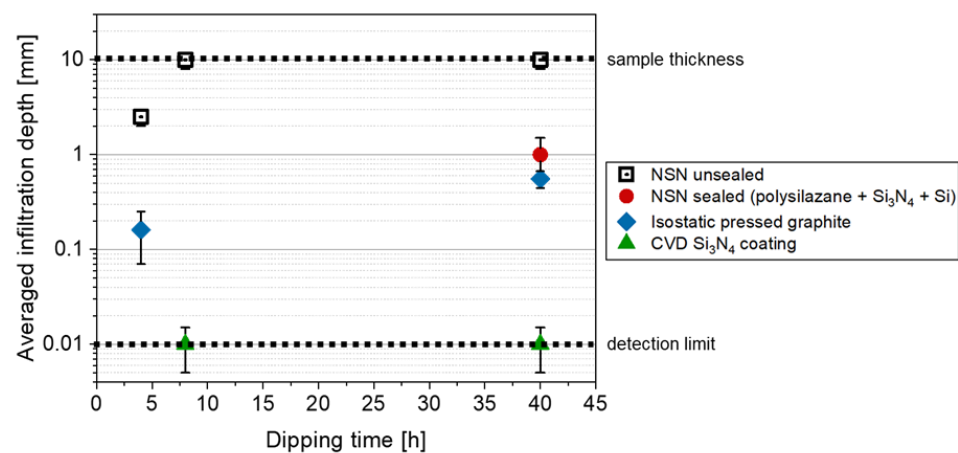


**Figure 3.** Averaged infiltration depth of liquid silicon after dipping in silicon melt between 4 h and 40 h.

First, the relatively dense graphite material (~11% porosity) shows only a minor infiltration depth of about  $600\ \mu\text{m}$ , even after 40 h in contact with liquid silicon. In combination with a sufficient mechanical strength of the chosen graphite material, this

prohibits any crack formation according to the occurring SiC formation within the infiltrated zone. The NSN material shows a significant higher affinity to silicon infiltration due to its high porosity of ~60 % combined with a good wettability by liquid silicon. In consequence, a 10 mm thick NSN sample was completely infiltrated by silicon melt, already after a dipping of 8 h. Therefore, the NSN material cannot be used as Cz crucible material in this untreated condition. However, if a polysilazane-based sealing coating is applied, a significant reduction of the infiltration depth after 40 h from >10 mm to about 1 mm could be achieved, which is close to the result of the graphite sample. Finally, in case of the CVD  $\text{Si}_3\text{N}_4$  coating on graphite, no infiltration in the range of the detection limit (<10  $\mu\text{m}$ ) could be observed at all, even at long time scale.

Beside the infiltration, also the dissolution behavior of the crucible (NSN, graphite) and coating (CVD  $\text{Si}_3\text{N}_4$ ) materials was examined by the dipping experiments. Residues of solidified silicon were removed from the dipped sample surface by an etching process and the averaged dissolved layer thickness was determined by vertical cross-sections. The results of the averaged dissolved layer thickness in dependence on the dipping time are shown in Figure 4.

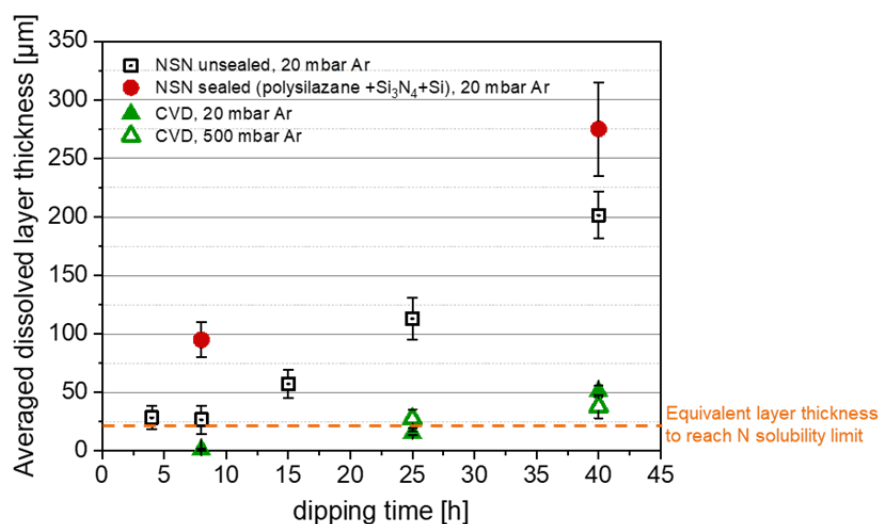


**Figure 4.** Measurement of dissolved layer thickness of NSN with and without polysilazane sealing as well as CVD  $\text{Si}_3\text{N}_4$ .

For unsealed NSN samples, an averaged dissolved layer thickness of about 25  $\mu\text{m}$  can be observed after a 4 h dipping, which nearly corresponds to the N solubility limit in the given silicon melt volume. With an increase of dipping time above 15 h also the averaged dissolved layer thickness increases. After 40 h nearly 200  $\mu\text{m}$  of the NSN material was dissolved in the silicon melt. NSN samples with an additional pore sealing (polysilazane +  $\text{Si}_3\text{N}_4$  + Si) reveal a higher dissolved layer thickness than the uncoated NSN material. This indicates that the sealing coating has a lower resistance to dissolution in liquid silicon than the NSN material itself. Nevertheless, the application of a pore sealing coating is basically indispensable to avoid complete crucible infiltration in case of CVD coating failure in terms of cracks or delamination.

In contrast to the NSN material, the CVD  $\text{Si}_3\text{N}_4$  coating exhibits a significant weaker material dissolution (see Figure 5), which predestines the CVD coating as ideal crucible functional surface coating. In case of 8 h of melt contact, the averaged dissolved layer thickness is in the range of the detection limit of 10  $\mu\text{m}$  and increases with increasing dipping time to 25  $\mu\text{m}$  for 25 h and 50  $\mu\text{m}$  for 40 h. This decelerated dissolution behavior compared to NSN can be connected to the high density and exceptionally low open porosity of the CVD  $\text{Si}_3\text{N}_4$ , of which properties have already been proposed to reduce dissolution in silicon melt [23]. Also at higher Ar pressures, in this case at 500 mbar (see Figure 4), the dissolution process of CVD  $\text{Si}_3\text{N}_4$  is rather slow. This could be beneficial if the Ar pressure

during the Cz process will be set to higher values (combined with the addition of nitrogen in the atmosphere), in order to increase the chemical stability of the  $\text{Si}_3\text{N}_4$  [17].

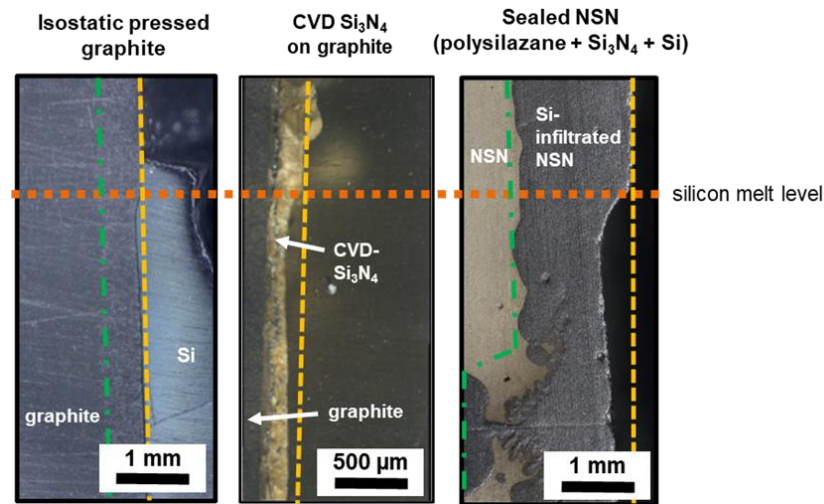


**Figure 5.** Vertical cross-section of isostatic pressed graphite samples, uncoated as well as with CVD  $\text{Si}_3\text{N}_4$  coating, and sealed NSN dipped in liquid silicon for 40 h. The orange dotted line marks the silicon melt level. The yellow dashed line represents the original sample surface and indicates the dissolution of material during melt contact. The green dot dashed line marks the silicon infiltration zone.

The dissolution of the uncoated isostatic graphite material during the dipping procedure was significantly lower than for CVD  $\text{Si}_3\text{N}_4$  coated graphite or NSN samples. In these cases, no dissolution, except directly below the Si melt level (see Figure 5), could be observed, meaning the averaged dissolved layer thickness must be below the detection limit of about  $10\ \mu\text{m}$ . This could be mainly attributed to the formation of a SiC layer [22,24], which leads to the passivation of the surface against further dissolution [25].

Besides the global material dissolution, which happens along the dipped sample surface, a more pronounced dissolution was observed at the region where silicon melt, graphite/ $\text{Si}_3\text{N}_4$  and the argon atmosphere coincide. This could be clearly seen at vertical cross-sections, which are exemplarily shown in Figure 5 for uncoated and CVD  $\text{Si}_3\text{N}_4$ -coated graphite as well as uncoated, sealed NSN samples after 40 h of melt contact.

The isostatic pressed graphite material shows the smallest maximum dissolved layer thickness in the triple area of about  $100\ \mu\text{m}$ , followed by the CVD  $\text{Si}_3\text{N}_4$  coating ( $150\ \mu\text{m}$ ) and sealed NSN ( $600\ \mu\text{m}$ ). As expected, this trend is in good correlation to the measurements of the averaged dissolved layer thickness over the whole dipped sample surface (see Figure 4).

This observation is mainly important for the prediction of the necessary CVD coating thickness. To ensure a closed CVD coating layer over the whole crucible surface for the entire silicon crystal growth process, the coating thickness must exceed the maximum dissolved layer thickness at the melt surface.

The phenomena of enhanced dissolution of different ceramic crucible and coating materials directly below the melt level are basically described in literature for iron containing melt systems [26] and also for quartz glass crucibles in contact with liquid silicon during a standard Cz growth process [27]. This effect is mainly caused by the Marangoni convection. By wetting the coating or crucible material surface by the silicon melt, the dissolution process is initiated, and a local change of melt composition and surface tension occurs. These gradients of concentration and surface tension are the driving forces for the Marangoni convection, and an enhanced mass flow advances the further dissolution of the crucible or coating material [26,28]. Furthermore, the depth of the resulting groove and, consequently, the dissolution rate of the crucible and coating materials seem also to depend

on the material properties. The dissolution rate  $V_{\text{dissolution}}$  [mm/h] by the Marangoni enhanced dissolution can be described with the following Equation (1) [26].

$$V_{\text{dissolution}} = 360 \cdot \frac{\rho_{\text{melt}}}{\rho_{\text{crucible}}} \cdot \beta \cdot (C_s - C_0) \quad (1)$$

where  $\rho_{\text{melt}}$  is the density of the silicon melt,  $\rho_{\text{crucible}}$  the density of graphite, NSN or CVD  $\text{Si}_3\text{N}_4$ ,  $\beta$  the mass transfer constant,  $C_s$  the saturation concentration of the dissolved phase (C or N) and  $C_0$  the initial concentration of the dissolved phase in the melt. This also explains basically the smallest maximum dissolved layer thickness in the triple area for CVD  $\text{Si}_3\text{N}_4$  compared to NSN. The CVD coating exhibits a significant higher density than the NSN material and, consequently,  $V_{\text{dissolution}}$  is reduced for the CVD coating. For graphite materials it must be considered that according to the use of a graphite crucible for the dipping experiments  $C_0$  of C may significantly higher than it is the case for N. This results in a decrease of the dissolution rate for the graphite samples.

Summarized, graphite and NSN with a pore sealing coating as well as CVD  $\text{Si}_3\text{N}_4$  showed material loss by dissolution and silicon melt infiltration only in a  $\mu\text{m}$  range during the dipping experiments. Due to the fact a Cz crucible typically exhibits a wall thickness in a range of 10 to 35 mm, the observed interaction of the crucible and coating materials with the liquid silicon is no crucial drawback for Cz application.

### 3.2. Long Term Crystallization Experiments in G0 Scale

#### 3.2.1. Performance and Durability of the Oxygen-Free Crucible Systems

In Figure 6, the top views on the crucible systems containing the resulting silicon crystal after the experiment are shown. For all crucible systems no melt leakage could be observed, and regular crystallization of silicon melt could be achieved. Further, all ingots stick to the crucible/coating system as expected due to the wettability of the graphite, NSN and CVD  $\text{Si}_3\text{N}_4$  materials towards the silicon melt. As expected, Fourier transformed infrared spectroscopy (FTIR) confirmed that no oxygen was incorporated into silicon ingots during the DS process.

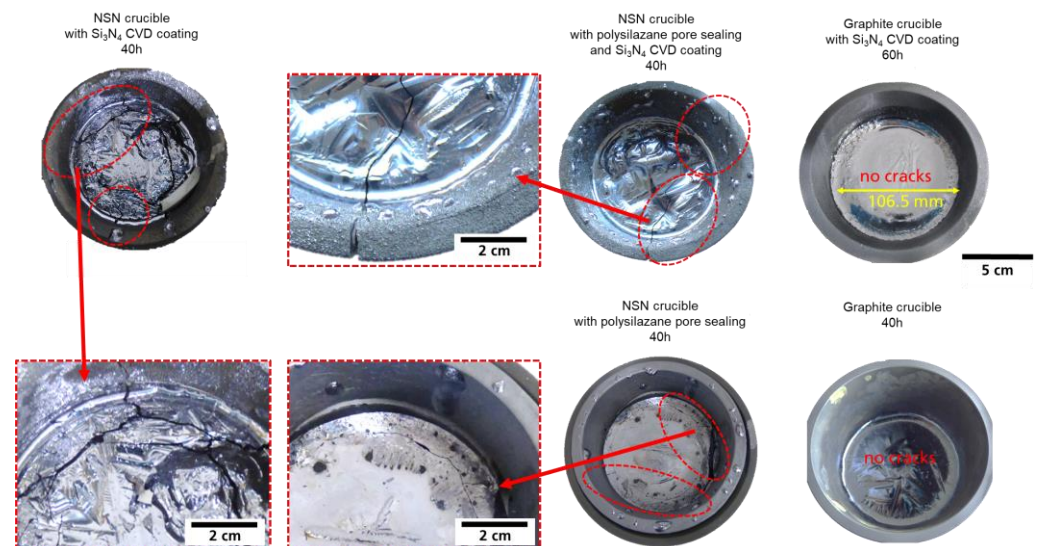


**Figure 6.** NSN and graphite-based crucible systems with silicon crystals after DS crystallization experiments with melt holding times of 40 h and 60 h. The red marks indicate crack formation in the crucible and the crystal.

#### NSN Crucibles

In case of NSN material, a significant crack formation in the crucibles and in the silicon crystals occurred, independent of the presence of a CVD  $\text{Si}_3\text{N}_4$  coating. Due to the absence

of melt leakage, and the fact that no strong Si infiltration was observed in cross-sections of the NSN crucibles (compare Figure 7), it can be assumed that the cracking was caused by thermal stresses occurring during the cooling after silicon crystallization. The stresses are induced by the difference in thermal expansion of solid silicon ( $\text{CTE} \sim 2.5 \times 10^{-6} \text{ K}^{-1}$ ) and the CVD coating/NSN crucible ( $\text{CTE} \sim 3.3 \times 10^{-6} \text{ K}^{-1}$ ). So basically, the mechanical strength of the NSN is not sufficient to absorb the thermal stresses resulting from the CTE mismatch. Although this may be in general no ideal basic condition for crucible application, it has to be considered that, in Cz growth, typically only a small portion of the residual melt solidifies in the crucible after the pulling of the Cz crystal is finished and therefore the CTE mismatch should not be such a severe issue.

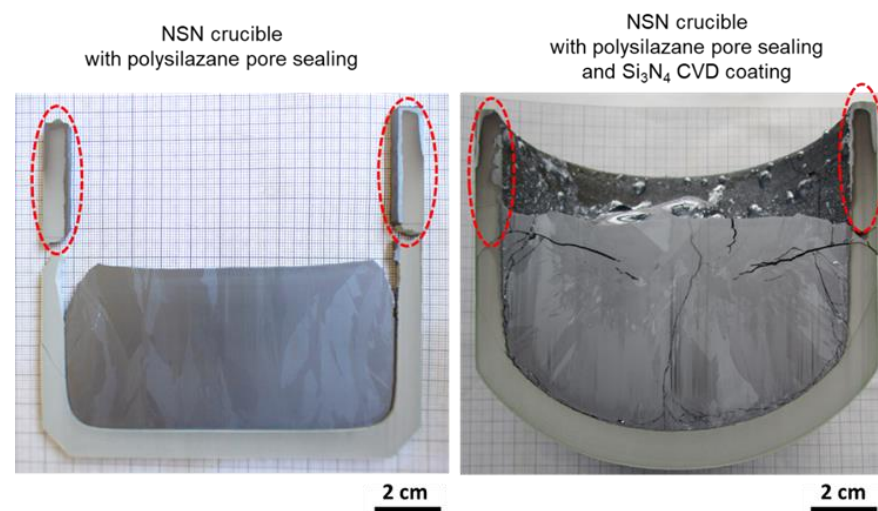


**Figure 7.** Vertical cross section of CVD coated NSN crucible bottom part after 40 h melt contact and silicon crystallization. In the marked areas silicon melt infiltration locally occurred.

By preparation of vertical cross-sections through the center of the crucible/crystal compound, the silicon infiltration in the different NSN crucible setups were investigated. For unsealed NSN crucible with CVD coating, no infiltration in coating or crucible could be detected. This underlines the ability of the CVD coating to inhibit direct melt contact with the crucible also on long time scales. Furthermore, no significant infiltration of liquid silicon in the two sealed NSN crucibles (with and even without CVD coating) could be observed below the silicon melt surface level (see Figure 7). The resulting infiltration depth on this site was even lower than it was previously observed for the bare shaped samples in the dipping experiments. This indicates that the pore sealing can be an effective tool to protect the NSN material from intense melt infiltration.

Above the melt level, a locally increased silicon infiltration depth was found at the top part of the crucibles in both tested NSN crucible configurations. This could be correlated to some micro-defects (cracks or voids) of the CVD coating and/or the sealing layer, which should be avoided by further optimization of the coating procedure.

### Graphite Crucibles

As shown in Figure 6, the visual inspection after the crystallization process of the graphite-based crucibles, with and without CVD coating, shows no obvious crack formation or deformation. Despite, the graphite material has a higher CTE ( $\sim 4.1 \times 10^{-6} \text{ K}^{-1}$ ) than the NSN/CVD materials, and in consequence, the CTE mismatch between crucible and the solidified Si is larger in this case; the mechanical strength of the used graphite material is sufficient to withstand the thermal stresses.

Silicon melt infiltration was not observed in the CVD-coated variant, showing again that the CVD coating acts as an effective barrier. In the uncoated case, only a small silicon melt infiltration of some hundreds of  $\mu\text{m}$  appears, as it was already observed in the dipping



experiments. However, the additional mechanical stresses, which occurs due to the SiC formation within the Si infiltrated zone, are obviously not high enough to induce crack formation in the graphite material. So, the chosen graphite material is suitable for the application as Cz crucible material, even in case of coating dissolution, delamination or failure. But it has to be noted that not all isostatic presses graphite types reveal high enough mechanical strength, as it was already presented in [19].

### CVD Coating

To evaluate the dissolution of CVD  $\text{Si}_3\text{N}_4$  coating during the crystallization experiments, a vertical cross-section of one coated graphite crucible (60 h melt contact) was prepared from various positions along the crucible wall and bottom. After removing the attached silicon by an etching process, the thickness of the still present CVD coating was measured (Figure 8).

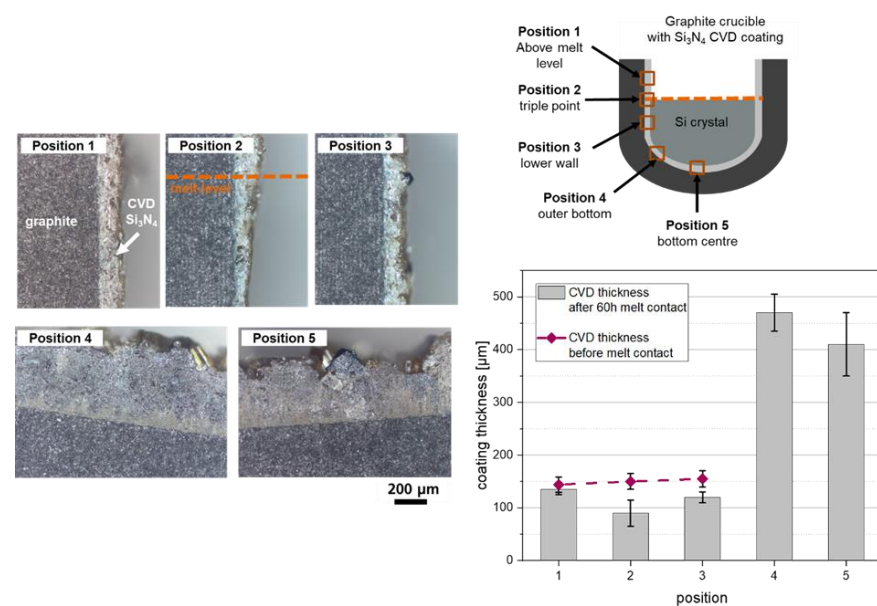


**Figure 8.** CVD coating thickness at different positions of a graphite crucible after 60 h melt contact and silicon crystallization. Because the measurement of coating thickness was only achievable by destructive methods, the CVD thickness before melt contact was determined at a crucible, which was coated with identical process condition as the crucible, used for silicon melting experiment.

Above the silicon melt surface level, a coating thickness of about  $135 \pm 10 \mu\text{m}$  is measured. Analogously to the dipping experiments, the lowest coating thickness ( $90 \mu\text{m} \pm 30 \mu\text{m}$ ) occurred directly below the contact point of the coating with the Si melt surface. Moving along the crucible wall downwards, the CVD thickness increases again up to  $120 \mu\text{m} \pm 10 \mu\text{m}$ , before it further increases in the spherical bottom region to  $>400 \mu\text{m}$ . Since the exact local CVD coating thickness before the melting experiment was unknown, values from destructive measurements of previously coated graphite crucibles were used for a rough estimation of the dissolved layer thickness. The results show that, in the region without Si melt contact, almost no dissolution exists, while in the region of the melt surface level the strongest dissolution of about  $50 \mu\text{m}$  has occurred. In the lower wall region, the coating thickness is only reduced by  $30\text{--}40 \mu\text{m}$ , which is on a similar level as in the dipping experiments ( $40\text{--}50 \mu\text{m}$  for 40 h, compare Figure 4). For the bottom region no reliable investigation of the CVD dissolution process could be achieved. The geometric limitation of flux, in combination with the high reactivity of the precursor gases, results in an increased variation of resulting CVD coating thickness at the bottom for each coating process.

Based on these results, a CVD  $\text{Si}_3\text{N}_4$  coating layer thickness of at least  $100\ \mu\text{m}$  should be applied for application in Cz growth to be sure that the coating is not completely dissolved.

### 3.2.2. Impact of Crucible/Coating Systems on Precipitate Formation in Grown Crystals

Within the frame of previous done short-term experiments (4 h melt holding time) [19], the application of a CVD  $\text{Si}_3\text{N}_4$  coating on the crucible has led to a significant reduction of  $\text{Si}_3\text{N}_4$  precipitates in the crystal volume in comparison to an experiment without the use of the CVD coating. This gives the hint that the coating could act as nucleation site for the  $\text{Si}_3\text{N}_4$  precipitates formed in the silicon melt supersaturated with nitrogen.

The same phenomenon could be also found in the new long-term experiments within uncoated and coated graphite crucibles. The observation in crystals grown within the NSN-crucibles was not possible due to the extended crack formation.

Corresponding investigations by IR transmission microscopy (Figure 9) reveals that, in the case of the non-coated graphite crucible (here, the nitrogen comes from  $\text{Si}_3\text{N}_4$  powder, which was intentionally added to the Si feedstock), the resulting crystal shows a significant formation of  $\text{Si}_3\text{N}_4$  precipitates in the central crystal volume and the top region.

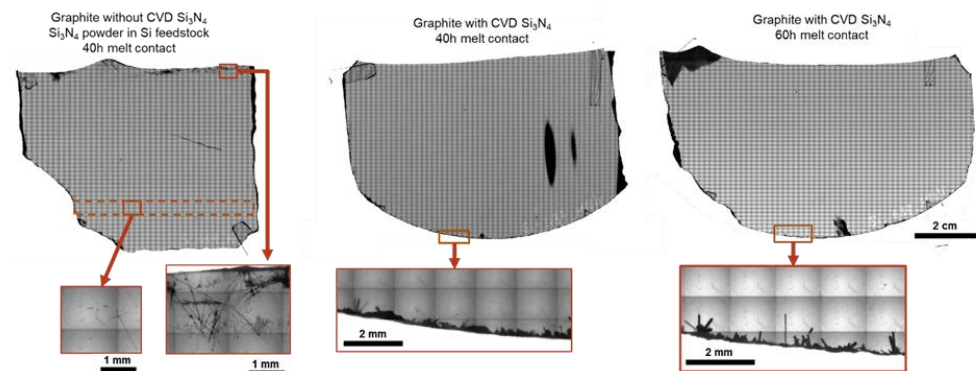


**Figure 9.** IR transmission microscopy images of vertical center slices from silicon crystals grown in graphite crucible with different nitrogen sources (CVD coating and  $\text{Si}_3\text{N}_4$  powder addition to feedstock).

In contrast, for both crystals grown in graphite crucibles with CVD coating (40 h and 60 h of melt contact),  $\text{Si}_3\text{N}_4$  needle-like structures were mostly detected directly at the interface between CVD  $\text{Si}_3\text{N}_4$  coating and silicon crystal. In the crystal volume no precipitates could be found, despite FTIR measurements also here show N contents closely above the solubility limit and therefore  $\text{Si}_3\text{N}_4$  precipitate formation could be expected. In this case, the heterogeneous nucleation on the CVD coating surface seems to be favored according to a reduced nucleation energy compared to the homogeneous nucleation of  $\text{Si}_3\text{N}_4$  precipitates in the silicon melt. Consequently, the CVD  $\text{Si}_3\text{N}_4$  coating could act as a nucleation site for nitrogen-related precipitates. A similar effect of preferred precipitate formation at a  $\text{Si}_3\text{N}_4$  based crucible coating used for DS growth of mc-Si ingots was already observed by Trempa et al. [29].

Additionally, a significant change in the resulting CVD  $\text{Si}_3\text{N}_4$  coating morphology after long time scale experiment (60 h) could be observed (Figure 10).

Besides the change in surface morphology, the  $\text{Si}_3\text{N}_4$  crystal size is also increased. This may indicate that, on the one hand, a recrystallization process of amorphous coating elements and/or a transition of  $\text{Si}_3\text{N}_4$  phase occurred during the silicon melt contact. On the other hand, also a deposition of parasitic precipitates on the CVD coating surface could take place due to the dissolution of  $\text{Si}_3\text{N}_4$  coating in liquid silicon, followed by an oversaturation of nitrogen in the melt [17].

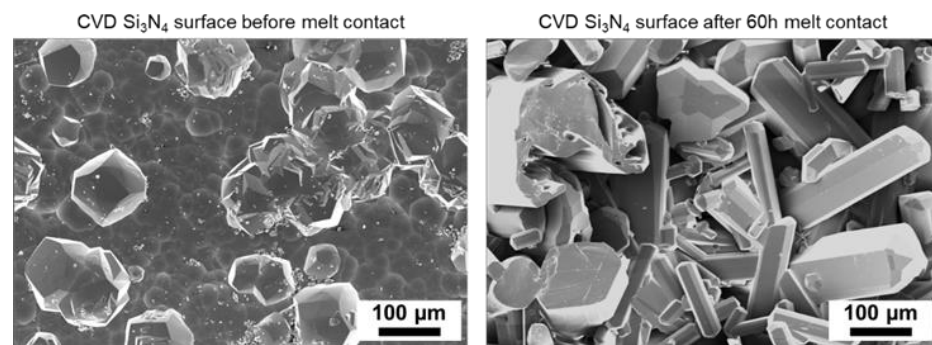


**Figure 10.** Morphology of CVD  $\text{Si}_3\text{N}_4$  surface before and after 60 h melt contact.

Nevertheless, even if all the experimental data support the thesis of the beneficial impact of the CVD  $\text{Si}_3\text{N}_4$  crucible coating on precipitate formation in lab scale directional solidification processes, the proof of concept must also be further demonstrated for real Cz growth process conditions.

#### 4. Conclusions

The basic evaluation of the long-term stability of oxygen-free crucible systems for the application in industrial Cz growth has shown that graphite and NSN-based crucible materials, in combination with a dense CVD  $\text{Si}_3\text{N}_4$  surface coating, have promising application potential. According to dipping experiments up to 40 h the CVD coating shows no infiltration and only weak dissolution by the silicon melt, which makes it attractive as a protection coating for the crucible base materials. But also, if the CVD coating would locally fail during process, the tested crucible base materials itself, such as isostatic pressed graphite with low porosity and appropriate mechanical strength as well as pore sealed NSN, have shown an excellent stability at this time scale, which is an important safety issue for industrial application.

These results are confirmed by laboratory scaled DS crystallization experiments with extended melt holding period up to 60 h. Also in this case, both crucible systems show a high robustness against the silicon melt.

With respect to the nitrogen contamination of the silicon melt, which is also a critical issue in Cz growth related to  $\text{Si}_3\text{N}_4$  precipitate formation and structure loss events, it could be found that the Si melt is always saturated with nitrogen by the partly dissolved CVD coating. However, all ingots grown in CVD-coated crucibles reveal no precipitates in the ingot volume. This indicates that the CVD  $\text{Si}_3\text{N}_4$  coating acts as nucleation site, which could enable the pulling of single crystalline Si ingots out of these crucible systems.

**Author Contributions:** Conceptualization, F.S. and M.T.; methodology, F.S. and M.T.; investigation, F.S., M.T., G.S., R.H., R.W., G.B. and P.M.; resources, G.S., P.G., R.W., G.B. and P.M.; writing—original draft preparation, F.S. and M.T.; writing—review and editing, G.S., R.H., P.G., R.W., G.B., P.M., C.R. and J.F.; visualization, F.S.; supervision, J.F.; project administration, M.T. and C.R.; funding acquisition, M.T. and C.R. All authors have read and agreed to the published version of the manuscript.

**Funding:** These research and development activities are carried out within the “X-treme” project funded by the Bavarian Research Foundation in Germany under contract number AZ-1317-17.

**Data Availability Statement:** Not applicable.

**Acknowledgments:** The project partners Alzchem Trostberg GmbH and Wacker Chemie AG are acknowledged for providing the  $\text{Si}_3\text{N}_4$ - and Si-powders.

**Conflicts of Interest:** The authors declare no conflict of interest.

## References

1. Schulze, H.J.; Öfner, H.; Niedernostheide, F.J.; Laven, J.G.; Felsl, H.P.; Voss, S.; Schwagmann, A.; Jelinek, M.; Ganagona, N.; Susiti, A.; et al. Use of 300 mm magnetic Czochralski wafers for the fabrication of IGBTs. In Proceedings of the 28th International Symposium on Power Semiconductor Devices and ICs (ISPSD), Prague, Czech Republic, 12–16 June 2016; pp. 355–358.
2. Kajiwara, K.; Harada, K.; Torigoe, K.; Hourai, M. Oxygen Precipitation Properties of Nitrogen-Doped Czochralski Silicon Single Crystals with Low Oxygen Concentration. *Phys. Status Solidi (A)* **2019**, *216*, 1900272. [[CrossRef](#)]
3. Hourai, M.; Nagashima, T.; Nishikawa, H.; Sugimura, W.; Ono, T.; Umeno, S. Review and Comments for the Development of Point Defect-Controlled CZ-Si Crystals and Their Application to Future Power Devices. *Phys. Status Solidi (A) Appl. Mater. Sci.* **2019**, *216*, 1800664. [[CrossRef](#)]
4. Kiyoi, A.; Kawabata, N.; Nakamura, K.; Fujiwara, Y. Influence of oxygen on trap-limited diffusion of hydrogen in proton-irradiated n-type silicon for power devices. *J. Appl. Phys.* **2021**, *129*, 025701. [[CrossRef](#)]
5. Schulze, H.-J.; Öfner, H.; Niedernostheide, F.-J.; Lükermann, F.; Schulz, A. Fabrication of Medium Power Insulated Gate Bipolar Transistors Using 300 mm Magnetic Czochralski Silicon Wafers. *Phys. Status Solidi (A)* **2019**, *216*, 1900235. [[CrossRef](#)]
6. Doi, H.; Kikuchi, N.; Oosawa, Y. Chemical vapour deposition coating of crystalline Si<sub>3</sub>N<sub>4</sub> on a quartz crucible for nitrogen-doped Czochralski silicon crystal growth. *Mater. Sci. Eng. A* **1988**, *105/106*, 465–480. [[CrossRef](#)]
7. Watanabe, M.; Usami, T.; Muraoka, H.; Matsuo, S.; Imanishi, Y.; Nagashima, H. Oxygen-Free Silicon Single Crystal Grown from Silicon Nitride Crucible. In *Semiconductor Silicon 1981: Proceedings of the 4th International Symposium on Silicon Materials Science and Technology*; Huff, H.R., Ed.; The Electrochemical Society: Pennington, NJ, USA, 1981; pp. 126–137.
8. Matsuo, S.; Imanishi, Y.; Nagashima, H.; Watanabe, M.; Usami, T.; Muraoka, H. Device made of silicon nitride for pulling single crystal made of silicon and method of manufacturing the same. patent EP 0065122, 24 April 1982.
9. Nakajima, K.; Morishita, K.; Murai, R.; Usami, N. Formation process of Si<sub>3</sub>N<sub>4</sub> particles on surface of Si ingots grown using silica crucibles with Si<sub>3</sub>N<sub>4</sub> coating by noncontact crucible method. *J. Cryst. Growth* **2014**, *389*, 112–119. [[CrossRef](#)]
10. Huguet, C.; Dechamp, C.; Camel, D.; Drevet, B.; Eustathopoulos, N. Study of interactions between silicon and coated graphite for application to photovoltaic silicon processing. *J. Mater. Sci.* **2019**, *54*, 11546–11555. [[CrossRef](#)]
11. Camel, D.; Cierniak, E.; Drevet, B.; Cabal, R.; Ponthenier, D.; Eustathopoulos, N. Directional solidification of photovoltaic silicon in re-useable graphite crucibles. *Sol. Energy Mater. Sol. Cells* **2020**, *215*, 110637. [[CrossRef](#)]
12. Hendawi, R.; Arnberg, L.; Di Sabatino, M. Novel coatings for graphite materials in PV silicon applications: A study of the surface wettability and interface interactions. *Sol. Energy Mater. Sol. Cells* **2022**, *234*, 111422. [[CrossRef](#)]
13. Schneider, V.; Reimann, C.; Friedrich, J.; Müller, G. Nitride bonded silicon nitride as a reusable crucible material for directional solidification of silicon. *Cryst. Res. Technol.* **2016**, *51*, 74–86. [[CrossRef](#)]
14. Bellmann, M.P.; Noja, G.; Ciftja, A. Eco-Solar Factory: Utilisation of Kerf-Loss from Silicon Wafer Sawing for the Manufacturing of Silicon Nitride Crucibles. In Proceedings of the 35th European Photovoltaic Solar Energy Conference, Brussels, Belgium, 24–28 September 2018; pp. 501–502.
15. Hendawi, R.; Ciftja, A.; Stokkan, G.; Arnberg, L.; Di Sabatino, M. The effect of preliminary heat treatment on the durability of reaction bonded silicon nitride crucibles for solar cells applications. *J. Cryst. Growth* **2020**, *542*, 125670. [[CrossRef](#)]
16. Lan, A.; Liu, C.E.; Yang, H.L.; Yu, H.T.; Liu, I.T.; Hsu, H.P.; Lan, C.W. Silicon ingot casting using reusable silicon nitride crucibles made from diamond wire sawing kerf-loss silicon. *J. Cryst. Growth* **2019**, *525*, 125184. [[CrossRef](#)]
17. Knerer, D. Verfahren und Vorrichtung zum Ziehen eines Einkristalls und Halbleiterscheibe aus Silizium. DE 102018210286 A1, 25 June 2018.
18. Hendawi, R.; Söndenå, R.; Ciftja, A.; Stokkan, G.; Arnberg, L.; Di Sabatino, M. Microstructure and electrical properties of multi-crystalline silicon ingots made in silicon nitride crucibles. *AIP Conf. Proc.* **2022**, *2487*, 130005. [[CrossRef](#)]
19. Sturm, F.; Trempa, M.; Schuster, G.; Götz, P.; Wagner, R.; Barroso, G.; Meisner, P.; Reimann, C.; Friedrich, J. Material evaluation for engineering a novel crucible setup for the growth of oxygen free Czochralski silicon crystals. *J. Cryst. Growth* **2022**, *584*, 126582. [[CrossRef](#)]
20. Mirkhalaf, M.; Yazdani Sarvestani, H.; Yang, Q.; Jakubinek, M.B.; Ashrafi, B. A comparative study of nano-fillers to improve toughness and modulus of polymer-derived ceramics. *Sci. Rep.* **2021**, *11*, 6951. [[CrossRef](#)] [[PubMed](#)]
21. Barroso, G.; Li, Q.; Bordia, R.K.; Motz, G. Polymeric and ceramic silicon-based coatings—A review. *J. Mater. Chem. A* **2019**, *7*, 1936–1963. [[CrossRef](#)]
22. Israel, R.; Voytovich, R.; Protsenko, P.; Drevet, B.; Camel, D.; Eustathopoulos, N. Capillary interactions between molten silicon and porous graphite. *J. Mater. Sci.* **2010**, *45*, 2210–2217. [[CrossRef](#)]
23. Chaney, R.E.; Varker, C.J. The Erosion of Materials in Molten Silicon. *J. Electrochem. Soc.* **1976**, *123*, 846–852. [[CrossRef](#)]
24. Eustathopoulos, N.; Israel, R.; Drevet, B.; Camel, D. Reactive infiltration by Si: Infiltration versus wetting: Viewpoint set no. 46 “Triple Lines”. *Scr. Mater.* **2010**, *62*, 966–971. [[CrossRef](#)]
25. Hoseinpour, A.; Safarian, J. Mechanisms of graphite crucible degradation in contact with Si–Al melts at high temperatures and vacuum conditions. *Vacuum* **2020**, *171*, 108993. [[CrossRef](#)]
26. Lian, P.; Huang, A.; Gu, H.; Zou, Y.; Fu, L.; Wang, Y. Towards prediction of local corrosion on alumina refractories driven by Marangoni convection. *Ceram. Int.* **2018**, *44*, 1675–1680. [[CrossRef](#)]
27. Chaney, R.E.; Varker, C.J. The dissolution of fused silica in molten silicon. *J. Cryst. Growth* **1976**, *33*, 188–190. [[CrossRef](#)]

28. Mukai, K. Wetting and Marangoni Effect in Iron and Steelmaking Processes. *ISIJ Int.* **1992**, *32*, 19–25. [[CrossRef](#)]
29. Trempa, M.; Reimann, C.; Friedrich, J.; Müller, G. The influence of growth rate on the formation and avoidance of C and N related precipitates during directional solidification of multi crystalline silicon. *J. Crys. Growth* **2010**, *312*, 1517–1524. [[CrossRef](#)]

**Disclaimer/Publisher’s Note:** The statements, opinions and data contained in all publications are solely those of the individual author(s) and contributor(s) and not of MDPI and/or the editor(s). MDPI and/or the editor(s) disclaim responsibility for any injury to people or property resulting from any ideas, methods, instructions or products referred to in the content.